The Hybrid Mineral Battery: energy storage and dissolution behavior of CuFeS$_2$ in a fixed bed flow cell

K. M. Deen*, E. Asselin

Department of Materials Engineering, University of British Columbia, Vancouver BC, V6T 1Z4, Canada

Supplementary Information

S – Experimental

Electrochemical testing in a three-electrode cell system

The electrochemical testing of individual electrode systems was carried out in a water jacketed three-electrode cell as shown in Figure S1. The potentiodynamic scans (PD) were obtained by applying potential (-1.5 V $\leq$ E$_{app}$ $\leq$ 1.2 V) versus open circuit potential (OCP) with a scan rate of 2 mV/s. The geometrical surface area of each (GF and composite) electrode was 14.4 cm^2. However, to adequately compare results, the current was normalized with the weight of the GF. A total of 25 mg of the CuFeS$_2$ + CB (4:1) mixture was used in the composite electrode. The electrochemical impedance spectra (EIS) were obtained by imposing a 5 mV AC potential amplitude over OCP of each electrode in their respective electrolytes (Table S1) and 100 kHz – 0.01 Hz frequency range was selected. Similarly, the cyclic voltammetry scans were obtained at various sweep rates (100, 80, 60, 40, 20, 15, 10, 5, 2 and 1 mV s^{-1}) to evaluate the kinetic response of the individual electrodes in their respective electrolytes – the combination of which we refer to as electrode systems.

Figure S1*: For electrochemical testing; three–electrode cell setup showing the arrangement of auxiliary, reference and working electrodes (magnified image represents the GF connected to graphite rod by conductive carbon paste)*

Construction of FBFC setup

A schematic diagram of the custom-made two electrode cell setup (FBFC) is shown in Figure S2. A cavity (10 mm in diameter and 10 mm deep) was made in the solid graphite rod to create flow channels and for the placement of electrode materials e.g. GF and GF–CuFeS$_2$ composite. The graphite felt (GF) and a composite (GF / CuFeS$_2$ + CB) electrode were compressed (to approximately 25% of their initial thickness) within the positive and negative compartments of the cell, respectively. In order to avoid air entrapment within the porous structure of both electrodes, these were pre-soaked in their respective electrolytes before inserting into the flow cavities. The two electrodes were separated by an expanded proton exchange membrane (PEM) (DuPont™ Nafion® XL). The conditioning/expansion of the PEM was carried out in boiling H$_2$O$_2$ (30%) solution followed by immersion in 2% H$_2$SO$_4$ solution at 60 ºC (2 h). The membrane was then rinsed several times in warm deionized (DI) water before storing in a plastic jar containing DI water for further use. The composite electrode (negative) was prepared by manually incorporating CuFeS$_2$ powder (80 wt. %) mixed with carbon black (CB) (20 wt. %) in the two halves of GF. The total mass of CuFeS$_2$ + CB used to prepare the composite electrode was 50mg. A 0.2 M H$_2$SO$_4$ solution (anolyte) was circulated within the negative compartment of the cell with a peristaltic pump in a closed loop. The catholyte (either 0.5M Fe^{2+} or 0.5M Fe^{2+} + 0.1M Cu^{2+} in 0.2M H$_2$SO$_4$) was pumped in the positive compartment. Both electrolytes were circulated continuously in their respective compartments of the FBFC at a constant flow rate of 7.5 ml/min. The temperature of the electrolytes was maintained constant (25 ± 1.0ºC) through external water jacketed reservoirs.

To remove dissolved oxygen, pure N_2 gas was bubbled for 1 h in both electrolytes before each experiment.
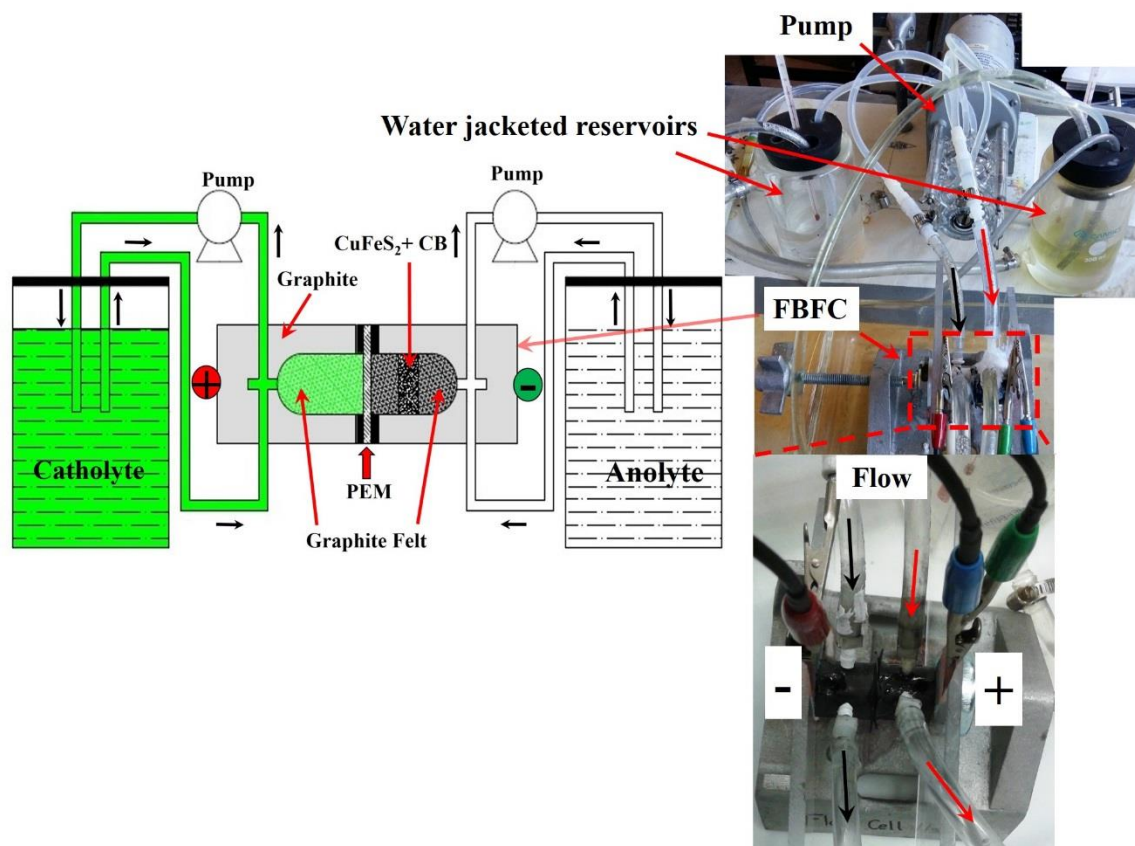

Figure S2: *Schematic diagram showing the design of the FBFC used in this study. The flow cell setup is also shown depicting the flow of electrolyte through water jacketed reservoirs by peristaltic pump and the cell connections*

Table S1: *Types of electrodes used as anode and cathode in the three-electrode cell assembly and tested in different electrolytes for electrochemical behavior investigations*

Type	Composition of the electrode	Electrolyte(s)
Anode	*GF / CuFeS$_2$+ CB (synthetic)	0.2M H$_2$SO$_4$
Cathode	GF	0.5M Fe^{2+} in 0.2M H$_2$SO$_4$
		0.5M Fe^{2+} + 0.1M Cu^{2+} in 0.2M H$_2$SO$_4$

*GF = Graphite felt, and CB = carbon black; Fe^{2+} and Cu^{2+} were added into solution by dissolving FeSO$_4$.7H$_2$O and CuSO$_4$.5H$_2$O salts in 0.2M H$_2$SO$_4$
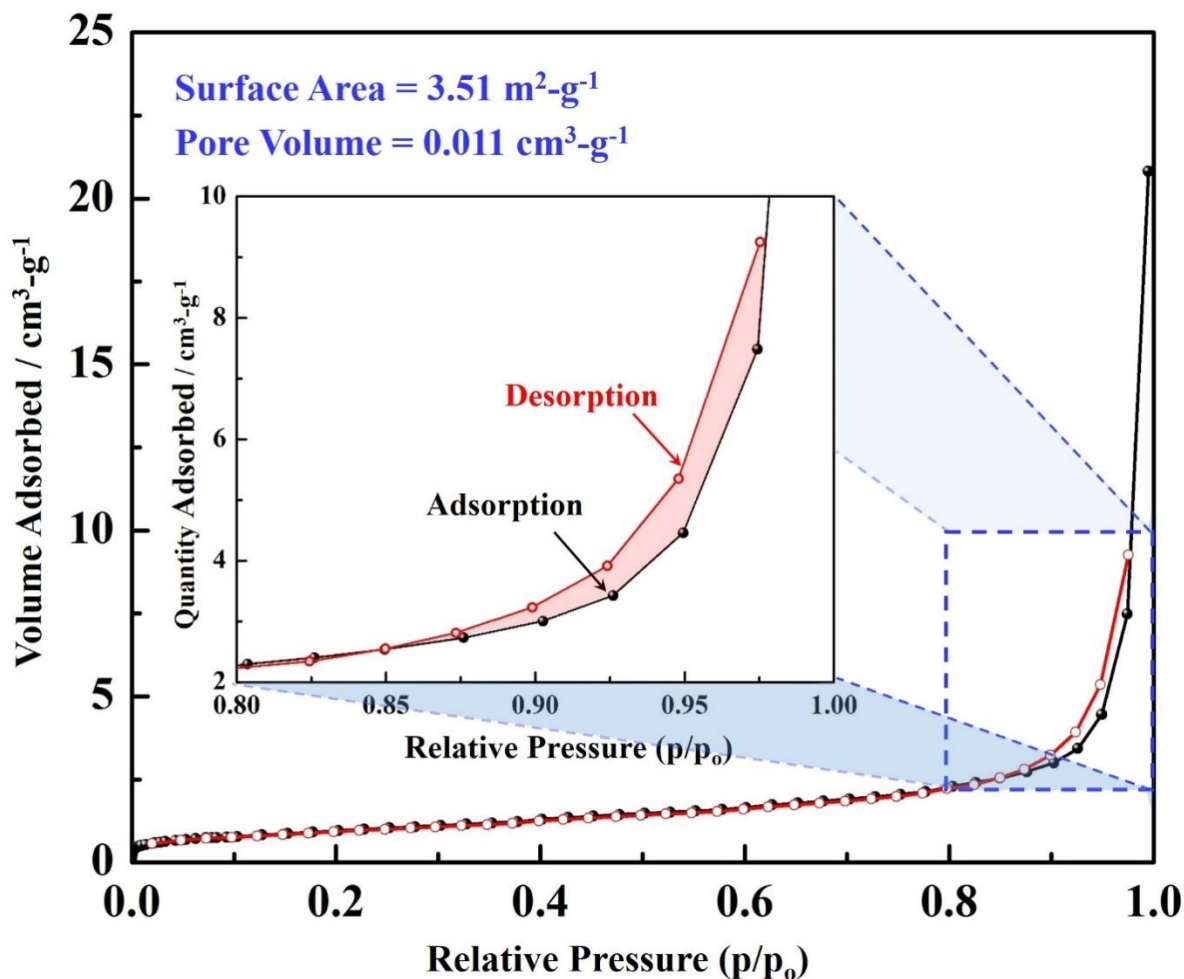
Figure S3: *Nitrogen adsorption/desorption isotherm of as–synthesized CuFeS$_2$ particles obtained at 77 K. The inset shows a magnified image of the hysteresis.*

Effect of Cu^{2+}addition on Fe^{2+}oxidation

The effect of Cu^{2+}addition on the catalytic oxidation of Fe^{2+} ions was studied electrochemically by applying a potential sweep at the rate of 5 mV s^{-1} to first charge (oxidation of Fe^{2+} into Fe^{3+}) the electrolyte on the surface of a GF electrode. N$_2$ was sparged for 30 min prior to each experiment and the temperature was kept constant at 25 ℃. After charging, and before each discharge (reduction of Fe^{3+} into Fe^{2+}) cycle, the potential of the GF electrode was relaxed at 0 V vs. OCP for 0, 1, 2, 4, 10, 20, 40 and 60 min, respectively in a sequential manner as presented in the Figure S4a. The electrolytes were freshly prepared before each experiment by mixing FeSO$_4$. 7H$_2$O (0.5M) into 0.2M H$_2$SO$_4$. The LSV discharge curves for the GF electrode in both the electrolytes (without and with the addition of Cu^{2+} species) are shown in figuresS4b and S4c, respectively. It

4

can be clearly seen in Figure S4d that the discharge current was high in Cu^{2+} containing solution even after prolonged delay at OCP. This increase in current even after extended delay during the discharging (negative scan) was likely directly related with the concentration of Fe^{3+} ions in the solution which were produced during the charging (positive scan) step and catalyzed by Cu^{2+} ions. This behavior also predicts the increased stability of Fe^{3+} ions in the electrolyte with the addition of Cu^{2+} species under applied conditions through reaction 7 (see *main text*). The reduction of Cu^{2+} during discharge/negative scan would produce intermediate '$Cu^+_{ads, GF}$' species at the surface of GF. This species would adsorb at the surface of GF by interacting with the surface functional groups and may increase the discharge current (reduction of Fe^{3+}) as confirmed from the experimental sequence. Zhang *et al.* [1] reported the effect of Cu addition on the oxidation of Fe^{2+} ions and proposed that Cu^{2+} could catalyze its oxidation in the presence of oxygen. In another study, Biniak *et al.* [2] described the mechanism of copper adsorption on activated carbon and the change in its oxidation state after interacting with the acid–base surface functionalities. Many other reports also described the cupric catalyzed oxidation of Fe^{2+} at high temperature and pressure in sulfate media [3, 4]. Based on the experimental evidence, and with the support of available literature, we have demonstrated the effect of cupric on the catalytic oxidation of ferrous on GF electrodes which may be beneficial for increasing the discharge current density, hence the energy density of the final FBFC device.
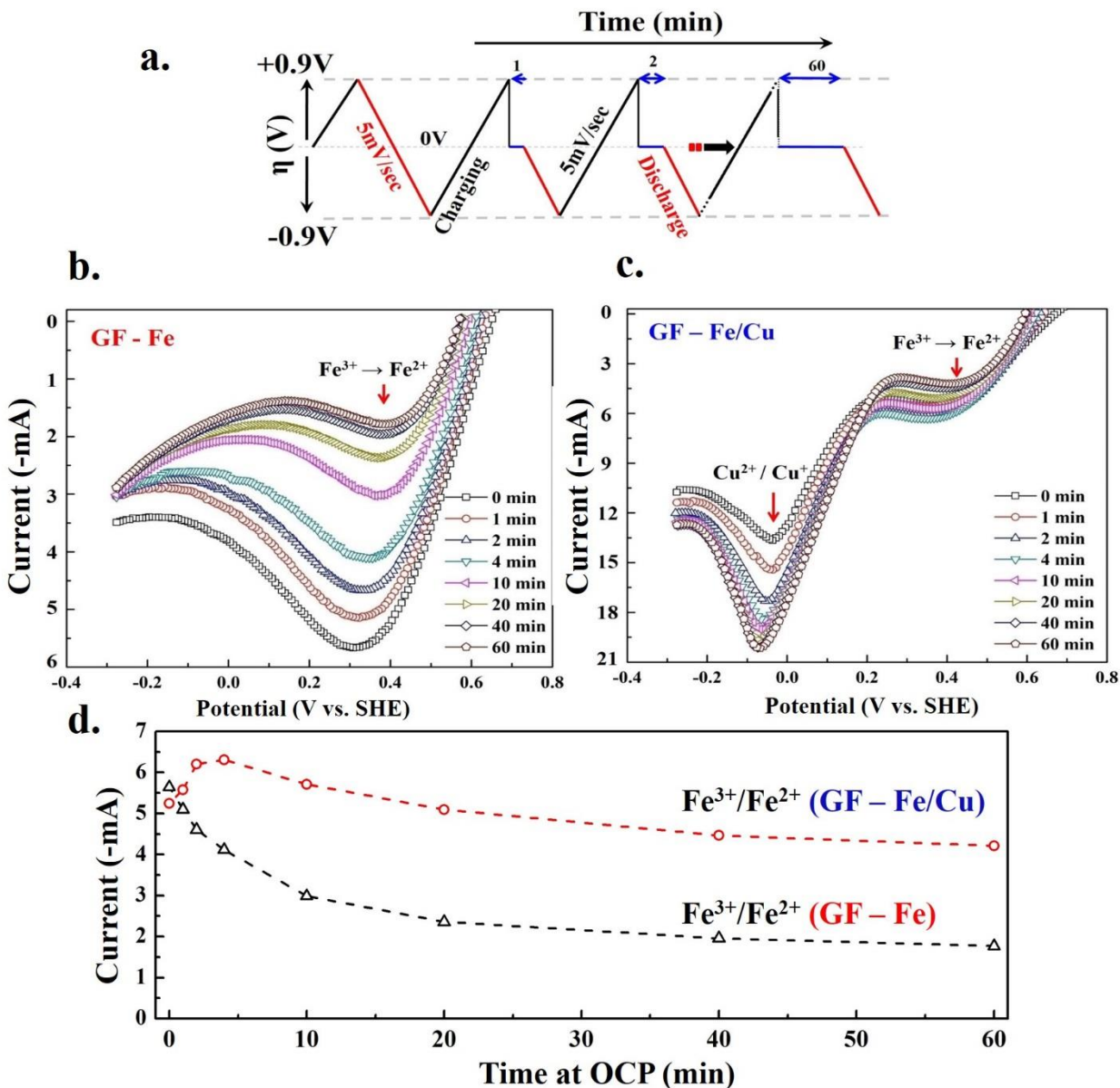
Figure S4: *Stability analyses of Fe^{3+} species in Cu^{2+}-containing solution at a GF electrode (a) Linear Scan voltammetry protocol applied for charging ($Fe^{2+} \rightarrow Fe^{3+}$) and sequential delay before discharging ($Fe^{3+} \rightarrow Fe^{2+}$) (b) The discharging current profile (reduction of Fe^{3+} into Fe^{2+}) after sequential delay form 0 to 60 min in 0.5M Fe^{2+} solution (c) discharge voltammograms for Fe^{3+} reduction in 0.1 M Cu^{2+} ions containing electrolyte, (d) peak current profile for Fe^{3+} reduction as a function of delay time between charging and discharging; (**Note:** For comparison the mass (187 mg) and geometrical surface area (14.4 cm^2) of GF electrode was the same in both cases. Only discharge curves are shown and potential reported is w.r.t. SHE)*

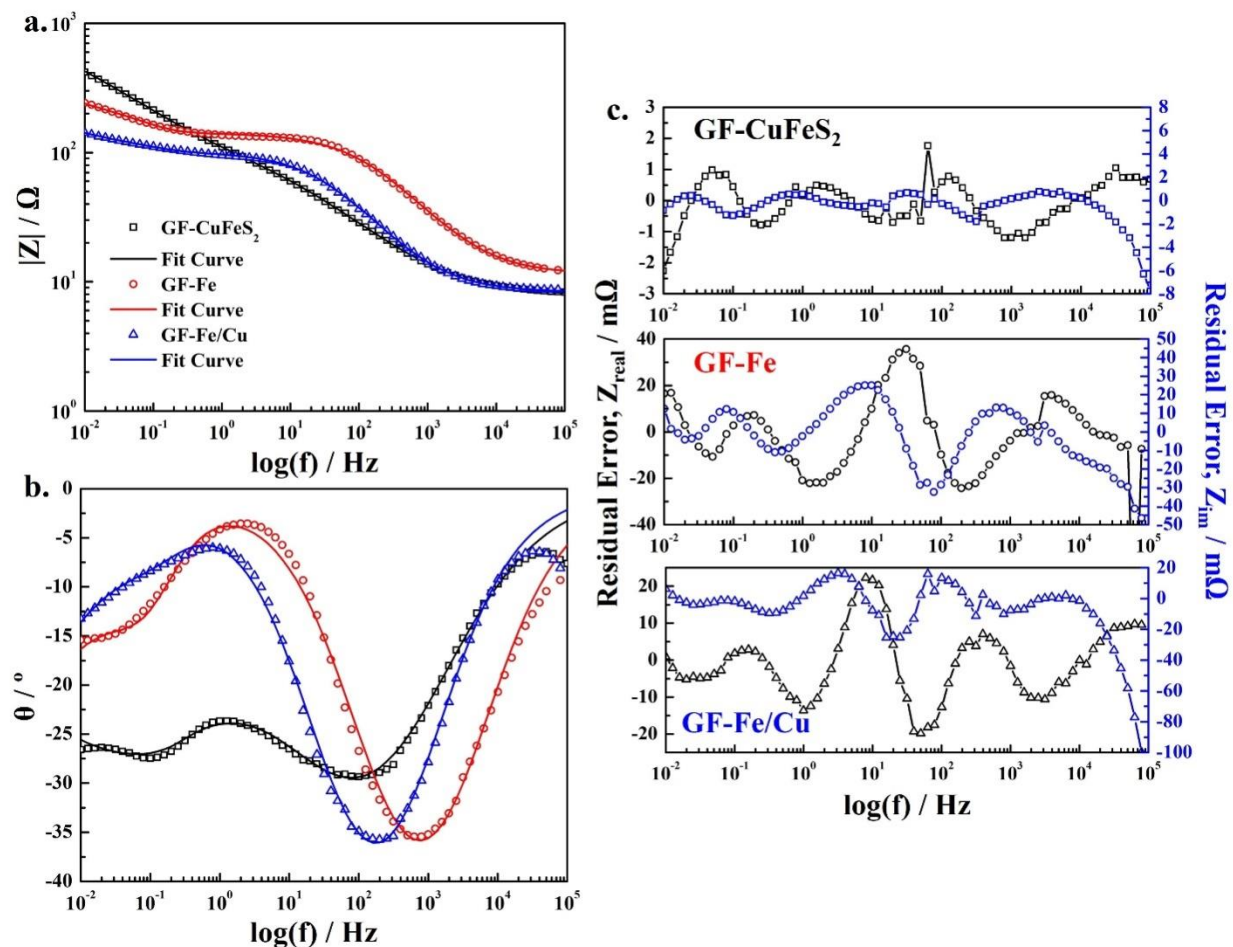*Impedance spectra of individual electrodes*

Figure S5*: (a) Bode plots (b) Phase angle (c) Residual error plots obtained after fitting the impedance spectra with equivalent electrical circuit. Note: The fitting was carried out through an iterative process and by adjusting the parameters of elements in the model editor (Echem Analyst 6.25 software; Gamry Instruments Inc.)*

Table S2: Impedance parameters evaluated from the experimental spectra at 0 V vs. OCP by applying 5 mV AC perturbation and simulating with the equivalent electrical circuit model

Parameters	GF – CuFeS$_2$ (Anode)	GF – Fe (Cathode)	GF – Fe/Cu (Cathode)
R_s (Ω)	7.77	11.13	8.31
Q_{dl} (μS s^{n1})	1119	93.9	330.5
n_1	0.54	0.67	0.68
R_{ct} (Ω)	84.74	130.2	93.11
Q_{ad} (mS s^{n2})	6.05	30.2	54.93
n_2	0.39	0.99	1.00
R_{ad} (Ω)	22.34	57.64	16.92
σ_B (Ω s$^{-1/2}$)	606.4	–	–
σ_w (Ω s$^{-1/2}$)	–	13.8	7.6
B (s$^{1/2}$)	1.99	–	–
Goodness of fit	2.0x10^{-4}	4.5x10^{-4}	4.9x10^{-4}

Element(s)	Conc. (Wt. %)
C	89.84
O	9.58
Na	0.22
Cl	0.36

Element(s)	Conc. (Wt. %)
C	82.76
O	14.82
S	0.76
Cl	0.56
Fe	1.11

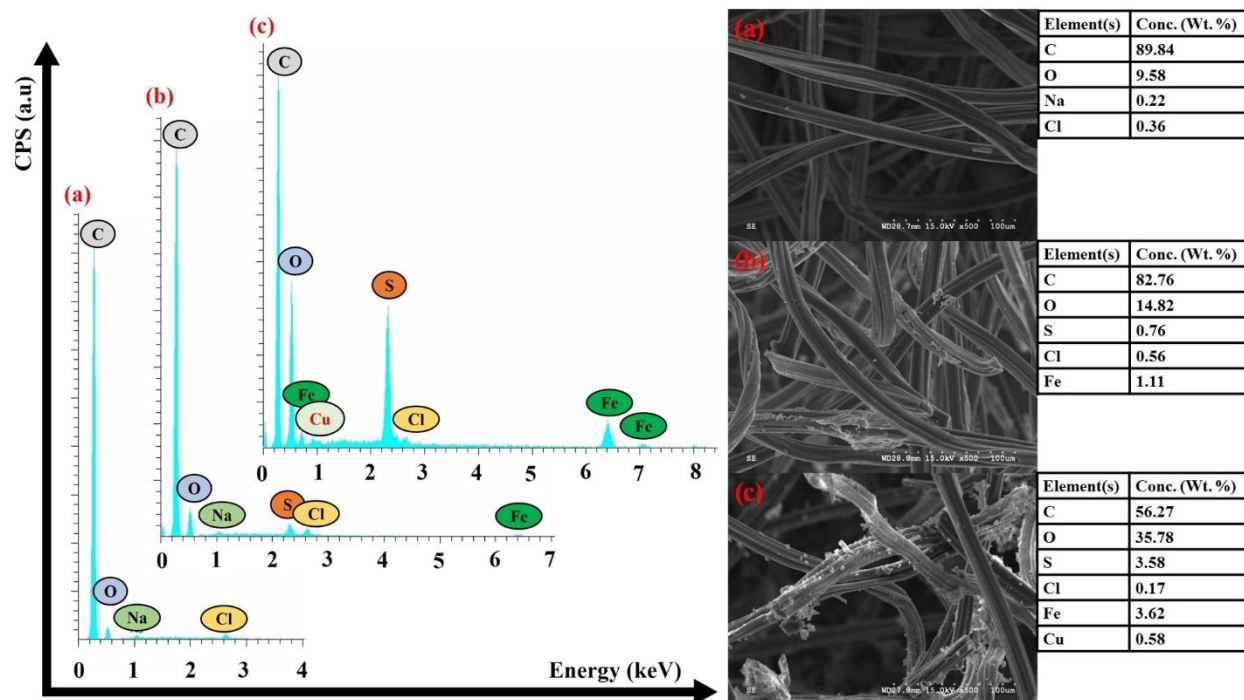| Element(s)	Conc. (Wt. %)
C	56.27
O	35.78
S	3.58
Cl	0.17
Fe	3.62
Cu	0.58

Figure S6: *SEM images and EDX analyses of the (a) as received GF (b) GF treated with 0.5M Fe^{2+}/0.2M H_2SO_4 solution and (c) GF treated in 0.5M Fe^{2+}/0.1M Cu^{2+}/0.2M H_2SO_4*
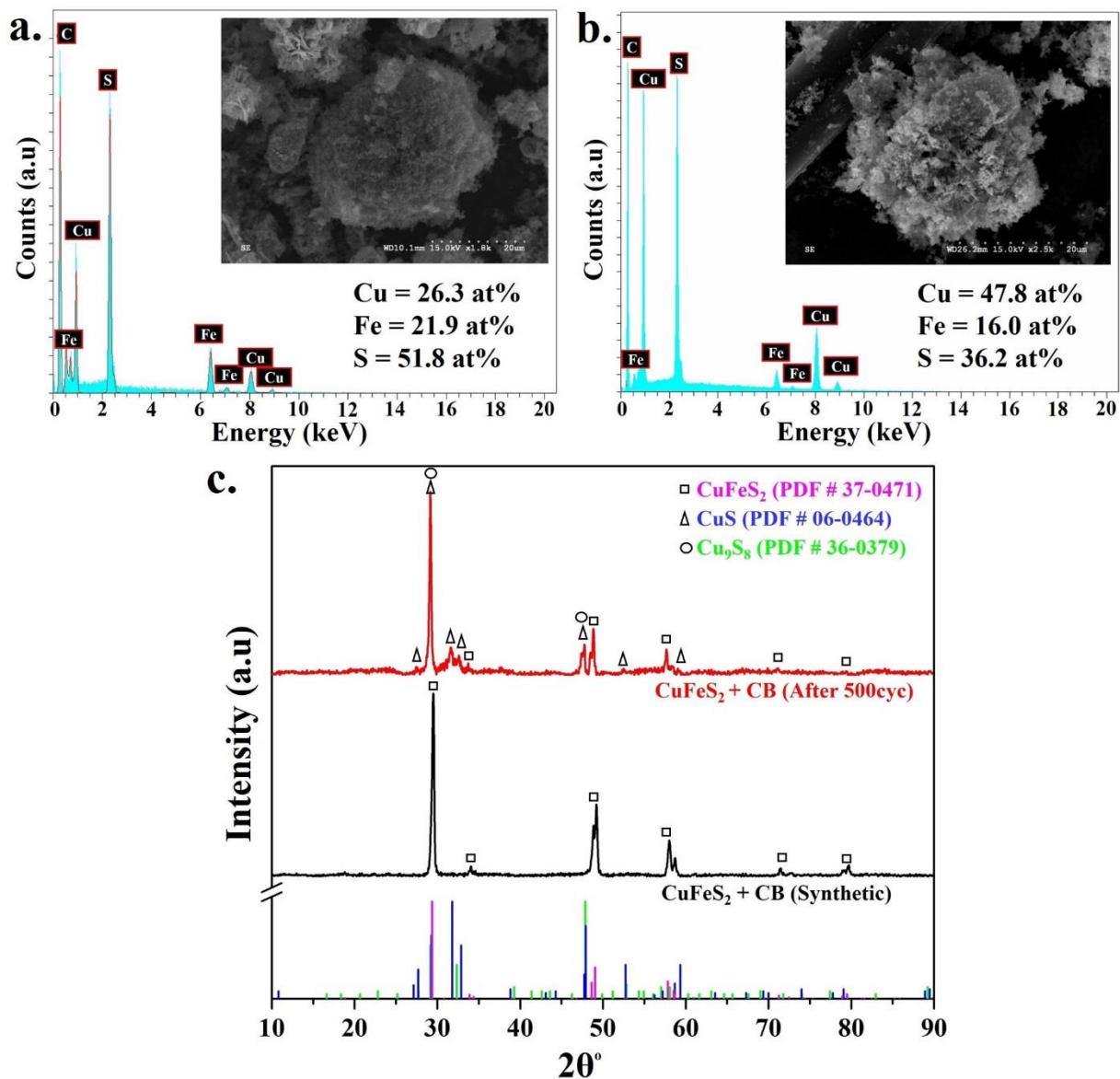
Figure S7: *Identification of any morphological, compositional and structural change in the CuFeS$_2$ before and after 500 GCD cycles in CFeCu cell system, SEM and EDX spectra of (a) as–synthesized, (b) and retrieved CuFeS$_2$, (c) comparing the XRD pattern of CuFeS$_2$ with the standard patterns*

In–situ pH variation during potentiostatic polarization

The pH of the $CuFeS_2$ slurry was measured during potentiostatic polarization as shown in Figure S8a. The two-electrode cell setup that was used is shown in the schematic diagram. The $CuFeS_2$ (80 wt. %) + CB (20 wt. %) slurry was thoroughly mixed and a 0.2 M H_2SO_4 solution was added to make a homogeneous slurry containing 20 wt. % solids. The measurements were made without stirring and the pH probe and counter electrodes were submerged in the semi–solid bed. The pH probe and counter electrode were manually adjusted to an approximate 3 mm distance from the working electrode.

The in–situ pH of the slurry at constant potentials (−1.0 V and +1.0 V) and the transient current were measured at different intervals as shown in Figure S8a and S8b, respectively. The initial pH of the slurry was measured to be 0.72 at OCP. The OCP was 0 V in this case since both counter and working electrode were graphite. During the change in cell potential (to −1.0 V), the pH of the slurry suddenly dropped to almost 0 indicating the abrupt migration of H^+ toward the negatively charged slurry particles. Under these conditions it is possible that H^+ could reduce the $CuFeS_2$ into intermediate species i.e. talnakhite ($Cu_9Fe_8S_{16}$) and bornite (Cu_5FeS_4) before converting these into chalcocite Cu_2S as indicated in reactions 2, 9 and 10 in the main text. The current was also found to increase (became less negative) due to the growth of a diffusion layer within the slurry, which approached a limiting current (Figure S8b). Under these transient conditions (charging process), the pH of the slurry increased to ~0.55 in 900 seconds.

It was interesting to see that the pH of the slurry shifted back toward the initial pH (~ 0.72) when the cell potential was reset to OCP. Following the charging process, the potential was shifted to +1.0 V (discharge) to evaluate the change in pH in this case. The current increased rapidly to a maximum of 35 mA and exponentially decayed before reaching a constant value (3.1 mA). This behavior corresponds to the oxidation of the $CuFeS_2$ and any intermediate species formed during the preceding charging process. The decrease in current and relatively low constant current also suggest that the decrease in dissolution rate is due to the formation of an Fe deficient and sulfide enriched surface film. The pH variation followed a similar trend to the current, and pH approached 1.96 upon sudden discharge attributed to the migration effect of cationic species in the opposite direction. The pH decayed to 0.94 during the initial 300 seconds and approached an almost constant value (0.89) in the next 600 seconds, which is most likely associated with the generation of oxidized species (Fe^{2+} and Cu^{2+} etc.) by the partial dissolution of $CuFeS_2$.
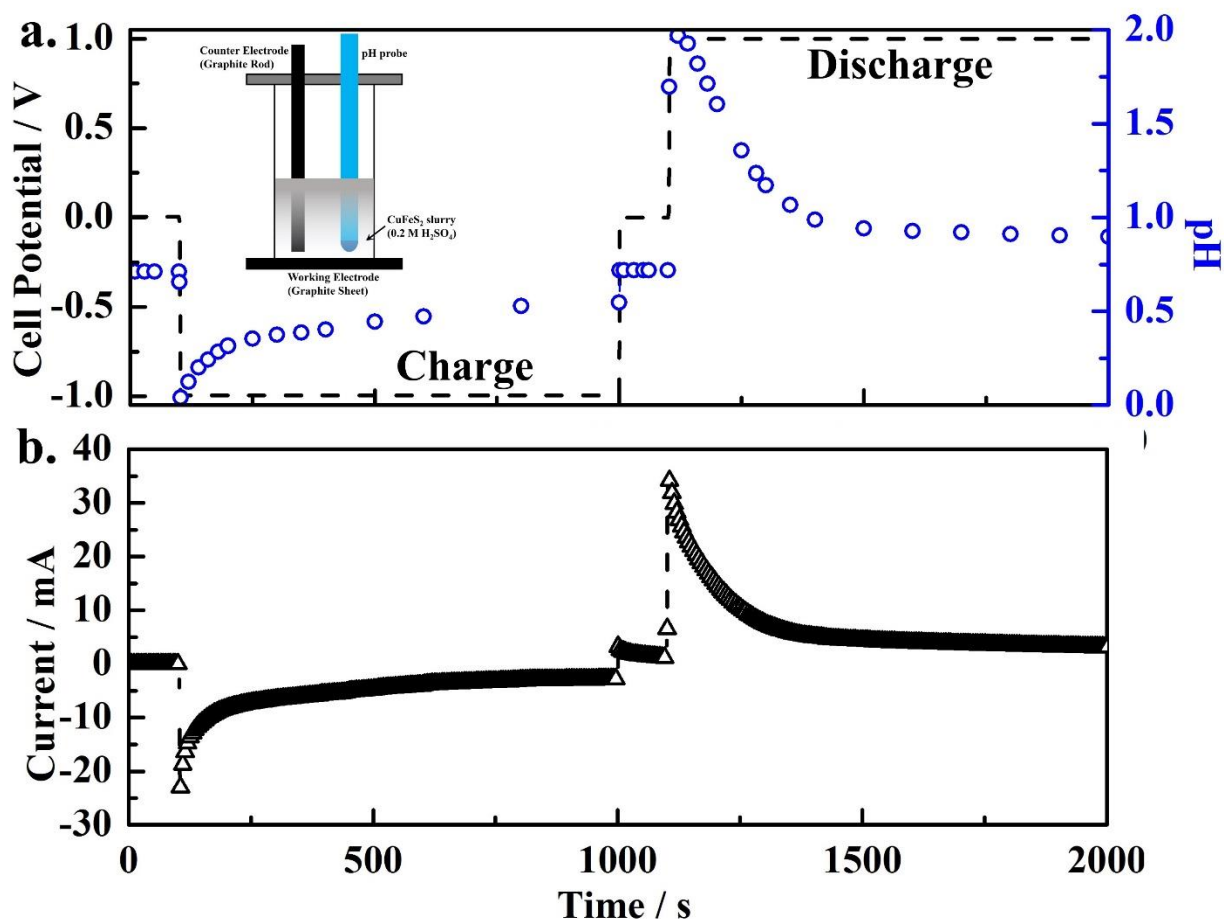
Figure S8: Potentiostatic polarization of CuFeS$_2$+ CB slurry (a) Variation of pH during charge (cell potential = −1.0 V) and discharge cycles (cell potential = 1.0), (b) Change in cell current during charge and discharge cycle (**Note:** Instead of composite electrode, only CuFeS$_2$ slurry in 0.2 M H$_2$SO$_4$ was used for pH measurements)

References

[1]. W. Zhang, D. M. Muir, P. Singh, Iron (II) oxidation by SO2/O2 in acidic media, Part II. Effect of copper, Hydrometallurgy 58 (2000) 117 – 125

[2]. S. Biniak, m. Pakula, G.S. Szymanski, A. Swiatkowski, Effect of activated carbon surface oxygen and/or nitrogen containing groups on adsorption of copper(II) ions from aqueous solutions, Langmuir, 15(18) (1999) 6117–6122

[3]. M. C. Ruiz, O. Jerez, R. Padilla, Kinetics of the cupric catalyzed oxidation of Fe^{2+} by oxygen at high temperature and high pressure, Min. Process. & Extractive Met. Rev. 37 (3) (2016) 160 – 167

[4]. D.B. Dreisinger, E. Peters, The oxidation of ferrous sulfate by molecular oxygen under zinc pressure-leach conditions, Hydrometallurgy 22 (1989) 101–119